

Extensional Stresses During Polymer Flow in Ducts

V. I. BRIZITSKY, G. V. VINOGRADOV, A. I. ISAYEV, and Y. Y. PODOLSKY, *Institute of Petrochemical Synthesis, USSR Academy of Sciences, Moscow, USSR 117912*

Synopsis

During the flow of high molecular weight, narrow-, and broad-distribution polybutadienes and polyisoprenes rheo-optical measurements were conducted of extensional stresses acting along the flow axis in the preentrance and entrance regions of the duct and of their subsequent relaxation in the duct. The extensional stresses increase in the preentrance region, reach their maximum values at a distance of two or three tenths of the duct width from its edges, and then relax. The position of the maximum extensional stress is independent of polymer characteristics, shear stresses in the duct, and shape of the entrance and dimensions of the rectangular duct. The dependence of the maximum extensional stress on the shear stress of the duct wall can be assumed to be linear for small values. The length of the stress relaxation zone depends on the shear stress at the duct wall and the molecular mass distribution. It is independent of the molecular masses in narrow-distribution polymers. For the polymers investigated, a generalized dependence was obtained for the reduced duct length over which the extensional stresses relax to zero from the reduced deformation rate. This dependence takes into account the characteristic polymer relaxation times and the value of the molecular mass of the chain between the fluctuation entanglement. A considerable decrease in the duct's length-to-width ratio leads to an increase in the maximum values of the extensional stresses. A decrease in the duct entrance angle causes a reduction in the rate of increase of extensional stresses, the maximum values, and the acceleration of the relaxation processes in the duct. A decrease in the ratio of the width of the preentrance region to the duct width leads to a reduction in the maximum in extensional stresses. It is shown that one of the causes for the instability of the polymer flow in the ducts can be the rupture of polymers due to their extension in the preentrance and entrance regions. Calculations were done that describe satisfactorily the relationship between the values of the maximum extensional stresses and the shear rate and stresses on the duct wall.

INTRODUCTION

During the flow of viscoelastic polymer systems in ducts, of great importance is the development of deformations in the preentrance and entrance regions of the duct where tangential stresses, the first normal stress difference, and extensional stresses act simultaneously. Evaluation of the tangential stresses and the first normal stress difference in the duct preentrance region was carried out comprehensively by Fields and Bogue¹ and Han and Drexler² using the rheo-optical method. It was shown that although tangential stresses and the first normal stress difference act simultaneously in most of the preentrance region, there are also zones where tangential stresses are nonexistent. On the basis of velocity profile measurements and observation of the stream lines, it has been shown³⁻⁵ that for polymer solutions and melts on transition from the reservoir to the duct, longitudinal deformations develop whose relative role increases with decreasing duct length. The strongest longitudinal deformations arise along the flow axis.

The indicated investigations, however, contain no quantitative information on the values of the extensional stresses arising in the preentrance region. A

method has been developed^{6,7} for indirect estimation of extensional stresses and longitudinal viscosity from the value of the pressure gradients at the entrance, which were measured by pressure gauges set up in the entrance region. These experiments showed that the dependence of longitudinal viscosity on extensional stresses, which was calculated from the pressure gradients in the entrance region, is in good agreement with the results of direct measurements by the method of assigning a constant extensional stress. The longitudinal viscosity as a function of the stress in relation to the nature of the polymer systems may be constant, or it may increase or decrease with increasing stress. Moreover, the value of the extensional stresses arising in the preentrance zone may reach and exceed 10^6 N/m², which corresponds, in the order of magnitude, to the rupture stress for linear polymers in the forced high-elastic state.⁸ Judging by this, the polymer may undergo a rupture even before entering the duct. It should be remembered that the extensional stresses measured by Cogswell^{6,7} are values averaged over the entire preentrance region of the duct and do not indicate the value of the extensional stresses in the zone of their maximum development, that is, on the flow axis, and the laws of their relaxation in the duct.

In estimating the extensional stresses arising during polymer flow in the preentrance and entrance regions of the duct, rheo-optical measurement may be of great importance. Here, we shall mention the investigation⁹ where it was noted that in solutions of poly(methyl methacrylate) in dibutyl phthalate and ethyl cellulose in benzyl alcohol, even at low shear stresses on the duct walls extensional stresses were revealed in the duct at a distance of tens of its width from the edge.

The present authors have undertaken a systematic study of extensional stresses along the flow axis during the passage of the polymer from the reservoir to the duct and inside the duct. In addition, the effect of the shape and relative dimensions of the preentrance and entrance zones of the ducts on the factors due to the extension and rupture of the polymers are discussed. The possibility of predicting the maximum values of extensional stresses if the flow curve and the dependence of the longitudinal viscosity on the deformation rate of the polymers are known is also demonstrated.

EXPERIMENTAL

Methods

Polymer flow was investigated on a previously described rheo-optical setup.¹⁰ A schematic representation of the working cell, containing a reservoir and a rectangular duct, is given in Figure 1. The optic axis of the setup is perpendicular to the drawing plane. The depth of the cell in the direction of the optic axis is 6×10^{-3} m. The dimensions of the cells used are given in Table I.

The pattern of isochromatic fringes obtained with light of wavelength $\lambda = 5460$ Å was recorded in the experiments. The velocity profiles and streamlines were registered by visually observing on the screen the motion of the particles introduced into the polymer. The particle diameter was $(3-5) \times 10^{-6}$ m.

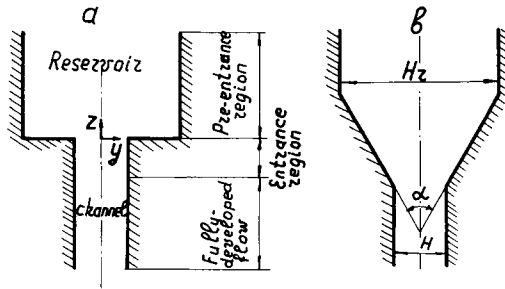


Fig. 1. Working cell diagram.

TABLE I
Dimensions of Rectangular Ducts

Cell no.	$H \times 10^3, \text{m}$	$L \times 10^3, \text{m}$	H_z/H	$\alpha, \text{degrees}$
1	2	28.7	6.25	180
2	1	40.0	12.0	180
3	6	42.0	2.5	180
4	2	30.0	6.25	120
5	2	30.0	6.25	105
6	2	30.0	6.25	45
7	2	30.0	6.25	30
8	2	5.97	6.25	180
9	2	10.0	6.25	180
10	2	4.2	6.25	180
11	2	2.31	6.25	180

Material

The polymers investigated were polybutadienes (PB) and polyisoprenes (PI) of narrow and broad molecular mass distribution. The specimen characteristics are given in Table II. According to Brizitsky et al.¹⁰ the stress-optical coefficient C of these polymers is equal to 3.3×10^{-9} and $1.9 \times 10^{-9} \text{ m}^2/\text{N}$ for PB and PI, respectively. All measurements were made at a temperature of $25^\circ \pm 0.5^\circ\text{C}$.

TABLE II
Characteristic of Polymers Studied

Polymer	$M_v \times 10^{-5}$	Isomeric composition				MMD M_w/M_n
		<i>cis</i>	<i>trans</i>	1,2	3,4	
Polybutadiene						
A	1.35	47	44	9	—	1.1
B	1.80	46	45	9	—	1.1
C	3.20	45	46	9	—	1.1
D	2.40	46	45	9	—	3.0
Polyisoprene						
E	3.75	79	15	—	6	1.14
F	5.75	69	25	—	6	1.02
G	8.30	85	10	—	5	1.12
H	6.00	88	8.2	—	3.8	2.4

RESULTS AND DISCUSSION

Figure 2 presents a typical pattern of isochromes (a) and stream lines (b) in the preentrance region and inside the duct for polymer B. It can be seen from Figure 2(a) that in the preentrance and entrance regions of the duct there are a number of isochromes. It is of importance that along the polymer flow axis the maximal tangential stresses are not equal to zero.

According to reference 11, the values of the principal stresses, σ_1 and σ_2 , are determined from the expressions

$$\begin{aligned}\sigma_1 &= \frac{\sigma_{11} + \sigma_{22}}{2} + \sqrt{\left(\frac{\sigma_{11} - \sigma_{22}}{2}\right)^2 + \tau_{12}^2} \\ \sigma_2 &= \frac{\sigma_{11} + \sigma_{22}}{2} - \sqrt{\left(\frac{\sigma_{11} - \sigma_{22}}{2}\right)^2 + \tau_{12}^2}\end{aligned}\quad (1)$$

where σ_{11} and σ_{22} are the normal stresses and τ_{12} is the shear stress. It follows that the maximum tangential stresses τ_{\max} are equal to

$$\tau_{\max} = \frac{\sigma_1 - \sigma_2}{2} = \sqrt{\left(\frac{\sigma_{11} - \sigma_{22}}{2}\right)^2 + \tau_{12}^2}\quad (2)$$

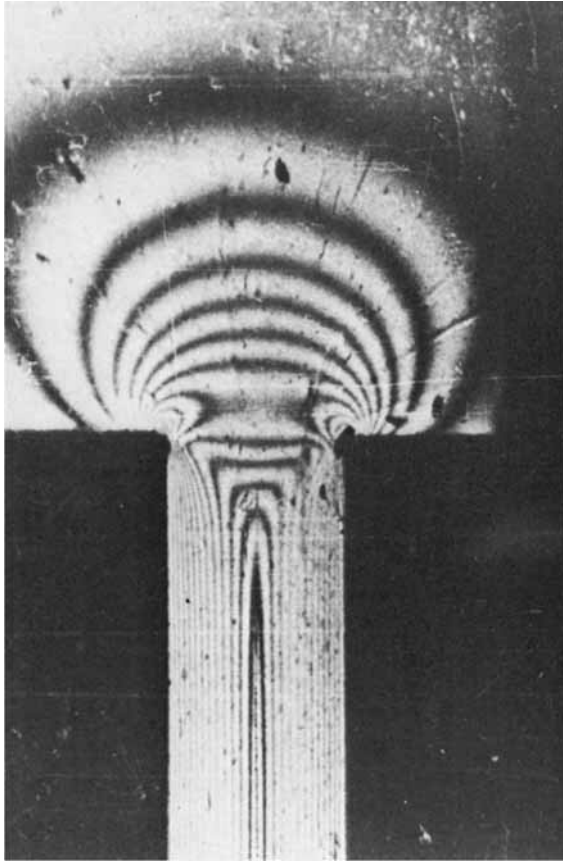


Fig. 2. Pattern of isochromes (a) and particle traces (b) in reservoir and inside duct no. 1 for sample B at $\tau_w = 1.33 \times 10^5$ N/m².

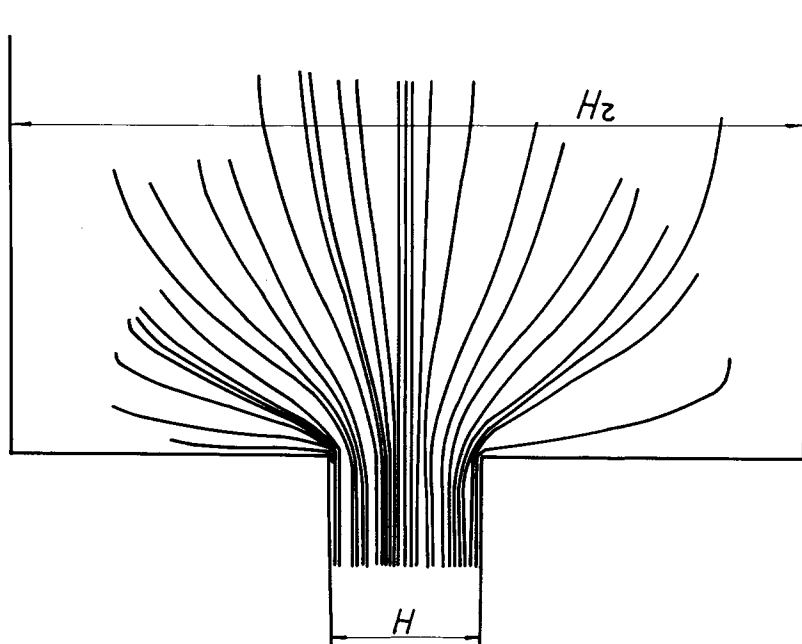


Fig. 2 (Continued from previous page.)

On the other hand, as can be seen from Figure 2(b) and from references 12 and 13, the streamlines at the duct entrance form a converging flow. Hence, in the preentrance and entrance regions the resultant flow rate has two components: the linear velocity v_{11} in the direction of flow and the transverse velocity component v_{22} . However, it is possible to single out on the flow axis an element satisfying the condition $v_{22} = 0$. For this element, the transverse deformation rate $\partial v_{22}/\partial y$ is also equal to zero. Therefore, one can also assume that on the flow axis the normal stress component σ_{22} is zero.

Considering that τ_{12} and τ_{22} are zero on the flow axis, it follows from eq. (2) that $\tau_{\max} = \frac{1}{2}\sigma_{11}$, i.e., only extensional stresses that are equal to the double maximum tangential stresses act along the flow axis. Thus, the recording of the isochrome pattern opens up a simple opportunity for determining the extensional stresses acting along the polymer flow axis. Here, there is a simple relationship between τ_{\max} and the parameters measured in the rheo-optical method¹¹:

$$\sigma_{11} = 2\tau_{\max} = \frac{n\lambda}{C \cdot W} \quad (3)$$

where n is the band number, λ is the light wavelength, C is the stress-optical coefficient, and W is the duct depth in the direction of the optic axis.

Figure 3 shows, for narrow-distribution PB and PI, the dependence of the extensional stress σ_{11} on the dimensionless length Z/H , i.e., the distance along the flow axis in terms of the duct width. To each plot in Figure 3 there corresponds a constant value of shear stress τ_w on the duct wall in the region of fully developed velocity profile. The positive values of Z/H refer to the preentrance region, and their negative values refer directly to the duct. The value of $Z/H = 0$ corresponds to the edges of the duct. Inspection of Figure 3 shows that in

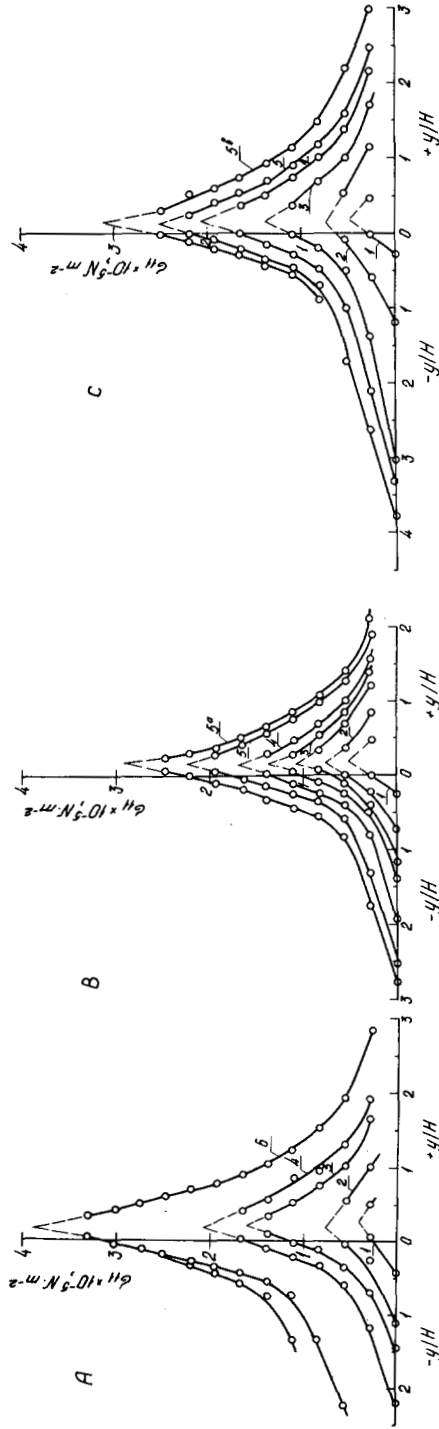


Fig. 3. Curves of distribution of extensional stresses along flow axis in reservoir and inside duct no. 1 for samples A, B, C, E, F, and G of narrow MMD at different shear stresses on duct wall, $\tau_w \times 10^4, N/m^2$: (1a) 4.2; (1) 4.3; (1b) 5.6; (2) 8.33; (3) 13.3; (4) 16.7; (5) 20.8; (5a) 22.0; (5b) 23.0; (6) 25.0.

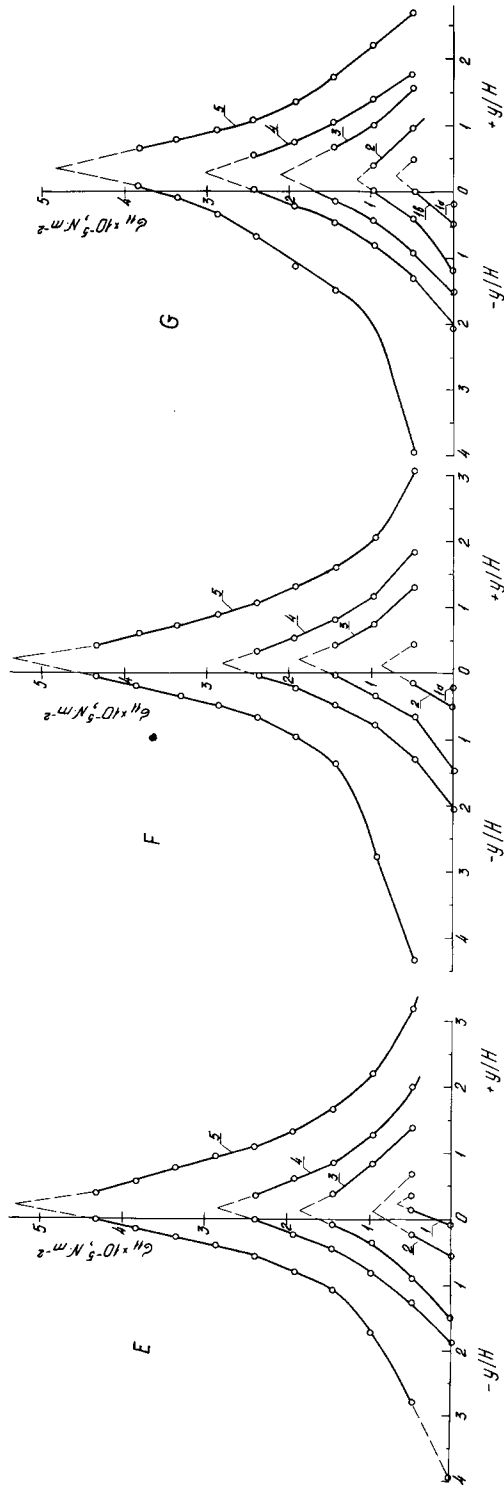


Fig. 3 (Continued from previous page.)

the preentrance region of the duct the extensional stresses increase, reaching a maximum; then a relaxation begins, which may terminate inside the duct.

When the dependences depicted in Figure 3 are represented in semilogarithmic coordinates (Fig. 4), then in the high-stress region the dependences $\sigma_{11}(Z/H)$ are practically linear, and this facilitates the determination of their points of intersection, i.e., the finding of the maximum values $\sigma_{11(\max)}$.

It was found that the maximum of extensional stresses is always located over the duct entrance at a distance of $(0.2-0.3) \times H$ from its edges and that the position of the maximum depends neither on the molecular mass of the polymers investigated nor on the value of the shear stresses on the duct wall in the region of developed flow. The position of the maximum of the extensional stresses on the flow axis can also be estimated from the data of reference 1. We assume that the first normal stress difference is equivalent to the extensional stresses. Calculation shows that at a distance of $0.2H$ from the duct edges the point of maximum extensional stresses according to the data of reference 1 is in full agreement with our data.

As regards the value of the highest extensional stresses as well as the reduced distance Z_0/H along the flow axis over which the extensional stresses relax to zero, they are determined unambiguously by the value of τ_w .

Figure 5 shows the variation in extensional stresses along the flow axis at different values of τ_w for specimens of broad-distribution PB and PI. A comparison of the data of Figures 3 and 5 indicates that the position of the maximum extensional stresses is independent of the molecular mass distribution. In addition, the molecular mass distribution strongly affects the rate of relaxation of the extensional stresses in the duct.

This is illustrated by Figure 6 for the investigated specimens of PB (a) and PI (b). The figure shows the reduced distances along the duct length over which the extensional stresses relax to zero. In the high molecular mass region, the dependence Z_0/H as a function of τ_w is, for narrow-distribution polymers, invariant of M . For broad-distribution polymers (upper curves) there is no such invariance. At the same values of shear stress τ_w , the values of Z_0/H for a polymolecular polymer may exceed more than threefold the values for narrow-distribution polymers. Moreover, at a given value of τ_w , the stress relaxation in broad-distribution polymers is greatly extended along the length of the duct.

It can be assumed that the dimensionless parameter Z_0/H is determined by the ratio of the deformation rate of the polymer in the duct and the characteristic relaxation time of the polymer. According to references 14 and 15, the characteristic relaxation time θ_0 is determined by the initial values of the Newtonian

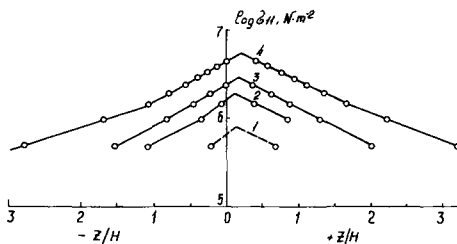


Fig. 4. Curves of distribution of extensional stresses along flow axis in reservoir and inside duct no. 1 for sample E at $\tau_w \times 10^5, \text{N/m}^2$: (1) 0.83; (2) 1.33; (3) 1.67; (4) 2.08.

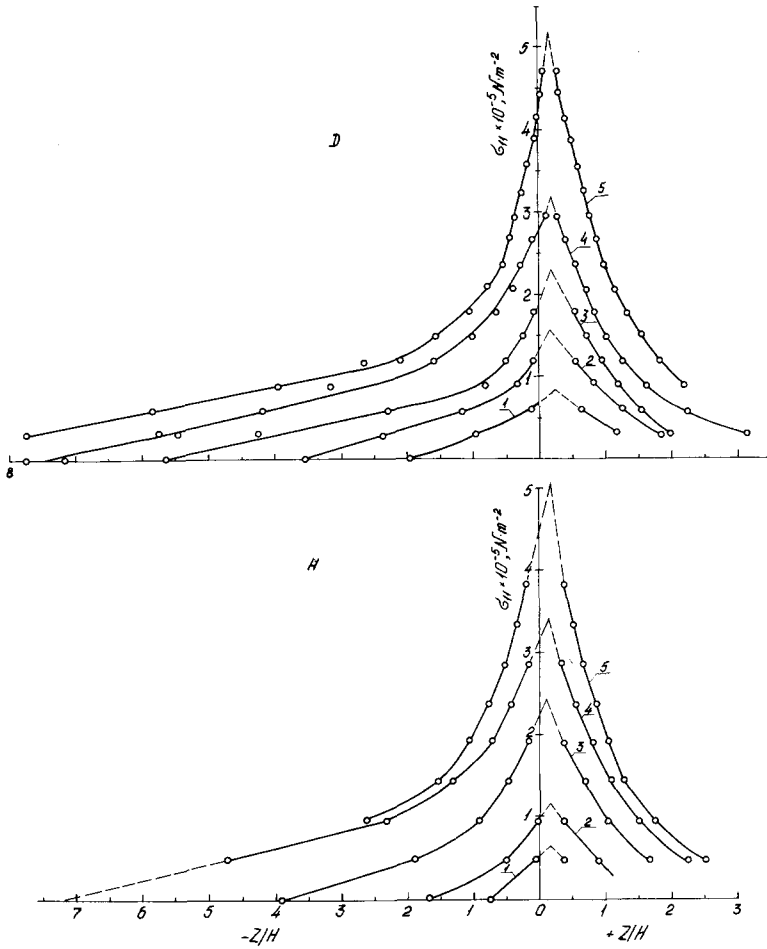


Fig. 5. Curves of distribution of extensional stresses along flow axis in reservoir and inside duct no. 1 for samples of broad-distribution D (a) and H (b) at different shear stresses on duct wall, $\tau_w \times 10^4$, N/m^2 ; (1) 5.1; (2) 9.8; (3) 14.1; (4) 21; (5) 25 for sample D; (1) 5.5; (2) 8.33; (3) 13.3; (4) 16.7; (5) 20.0 for sample H.

viscosity η_0 and the high-elasticity modulus G_e^0 . Since in the high molecular mass region in narrow-distribution polymers G_e^0 is independent of the molecular mass, $\theta_0 \sim M^\alpha$, where α is an index characteristic of the dependence $\eta_0 = f(M)$ in the high- M region. In narrow-distribution polymers, for each given value of τ_w the corresponding value of the shear rate $\dot{\gamma}_w$ is inversely proportional to M^α . Hence, the product of the characteristic relaxation time and the deformation rate at a given value of τ_w is a constant. This explains the invariance of Z_0/H to molecular masses for each given constant value of τ_w , whereas for broad-distribution polymers the value $\dot{\gamma}\theta_0$ is always greater than for narrow-distribution polymers. Therefore, the dependence of Z_0/H on τ_w for broad-distribution polymers is always higher than for narrow-distribution ones (see Fig. 6).

The value of Z_0/H must be associated with the conformational characteristic of the polymer chain. This characteristic is determined by the ratio of the second moment of the distance between the ends of the molecule, $\langle r^2 \rangle$, and the number of independent segments, N . For a free-jointed chain this ratio is proportional to l^2 , where l is the segment length.¹⁶

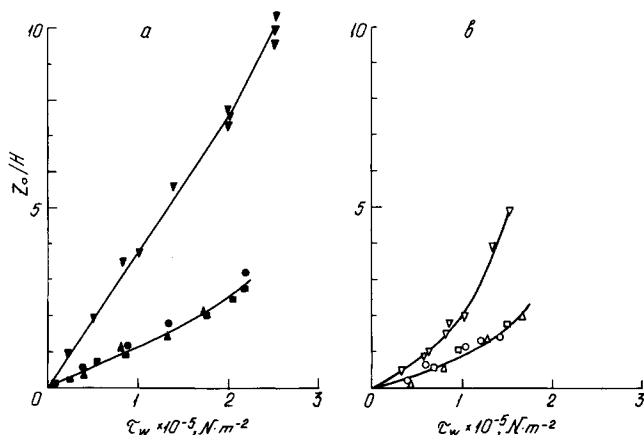


Fig. 6. Dependence of dimensionless distance Z_0/H (corresponding to complete relaxation of extensional stresses) on shear stress on duct wall for polybutadienes (a): (\blacktriangle) A; (\blacksquare) B; (\bullet) C; (\blacktriangledown) D; and for polyisoprenes (b): (\triangle) E; (\square) F; (\circ) G; (\triangledown) H.

The distance over which the extensional stresses drop to zero must be determined by the size of the segment, which can be judged by the value of M_e equal to the mass of the portion of the chain between the entanglements. Indeed, it can be seen from Figure 7 that all the polymers investigated are described by a unique dependence of $(Z_0/H) \cdot M_e^2$ on $\dot{\gamma} \cdot \theta_0$. When plotting this dependence, use was made of values of M_e equal to 2800 and 7000, respectively, for polybutadienes and polyisoprenes.¹⁷ The values of the initial high-elasticity modulus used in determining the characteristic relaxation time are borrowed from reference 18.

It has been shown above that there is an unambiguous relationship between $\sigma_{11(\max)}$ and τ_w . Let us first consider the possibility of calculating this dependence. To compute $\sigma_{11(\max)}$, we assume that during the passage of the polymer from the reservoir to the duct there is, on the flow axis, a stationary regime of extensional deformation. Then $\sigma_{11(\max)} = \dot{\epsilon} \cdot \lambda$, where $\dot{\epsilon}$ is the longitudinal deformation rate and λ is the longitudinal viscosity. We also assume that the extensional deformations of some volume element of the polymer with a linear dimension a , located on the flow axis, occur in the entrance region because of the difference in the motion velocity of its ends, $v = v_1 - v_0$, where v_1 is the polymer velocity in the region of the duct edges and v_0 is the polymer velocity along the reservoir axis in the region of the fully developed flow.

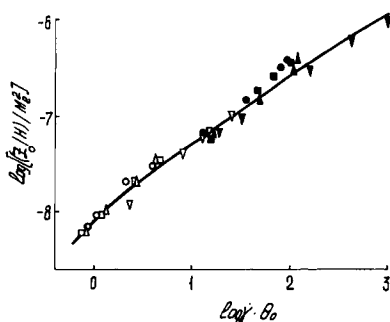


Fig. 7. Master curve of reduced length over which extensional stress relaxes to zero on reduced deformation rate for polybutadienes and polyisoprenes. Notation same as in Figure 6.

As can be seen from Figure 8, the velocity profile at the duct edges has a near-rectangular shape (i.e., $v_1 = Q/W \cdot H$). On the other hand, according to reference 10, narrow-distribution polybutadienes and polyisoprenes show during the flow a near-Newtonian behavior over a rather wide range of shear stresses, which makes it possible to calculate v_0 in a reservoir of rectangular cross section:

$$V_0 = 1.5k \frac{Q}{w \cdot H_r} \tag{4}$$

where Q is the volume output per second. It can be seen that eq. (4) is similar in form to the corresponding formula for calculating v_0 in the case of flow of a Newtonian liquid through a rectangular slot of infinite depth¹⁹ with a correction K for the perturbing effect of the front and back walls of the reservoir.

The value of extensional deformation of a unit volume of the polymer during the passage from a reservoir of width H_r into a duct of width H is according to Hencky, $\epsilon = \ln H_r/H$. Since the duration t of extensional deformation is $a/\Delta V$, we have

$$\dot{\epsilon} = \epsilon/t = \frac{Q(H_r - 1.5K \cdot H) \ln H_r/H}{W \cdot H \cdot H_r \cdot a} \tag{5}$$

According to the data of Vinogradov,⁸ the narrow-distribution polybutadienes and polyisoprenes obey the Trouton rule $\lambda = 3\eta_0$, where η_0 is the initial Newtonian viscosity. Consequently,

$$\sigma_{11(\max)} = \frac{3\eta_0 Q(H_r - 1.5K \cdot H) \ln (H_r/H)}{W \cdot H \cdot H_r \cdot a} \tag{6}$$

According to Brizitsky et al.,¹⁰ the volume output of a polymer through a rectangular slot can be expressed in terms of the shear rate on the duct wall ($\dot{\gamma}_w$):

$$Q = \frac{W \cdot H^2}{6k'} \cdot \dot{\gamma}_w \tag{7}$$

where k' has the same meaning as the coefficient k in eq. (4). Thus,

$$\begin{aligned} \sigma_{11(\max)} = \lambda \cdot \dot{\epsilon} &= \frac{\ln (H_r/H)(H_r - 1.5KH)H\eta_0 \cdot \dot{\gamma}_w}{2k' \cdot H_r \cdot a} \\ &= \frac{H \ln (H_r/H)(H_r - 1.5K \cdot H)\eta_0 \cdot \tau_w}{2k' \cdot H_r \cdot \eta_0 \cdot a} \end{aligned} \tag{8}$$

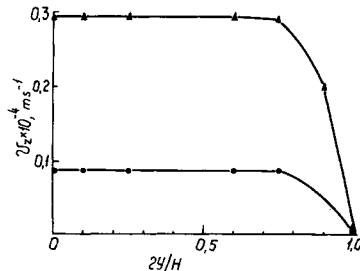


Fig. 8. Profile of stream velocities in plane of edges of duct no. 1 at $\tau_w \times 10^4, N/m^2$: (●) 4.9; (▲) 13.5.

The numerical values of the coefficients k and k' are 1.312 and 1.246 for the reservoir $(6 \times 12.5) \times 10^{-6} \text{ m}^2$ and the duct $[Wh = (6 \times 2) \times 10^{-6} \text{ m}^2]$, respectively.

As can be seen from eq. (8) for polymers showing Newtonian behavior, the maximum of the extensional stresses along the flow axis during the passage from the reservoir into the duct depends linearly on the shear rate and stress on the duct wall and is determined by the ratio of the sides of the rectangular section of the reservoir and the duct.

Figures 9 and 10 show respectively the dependences of the value of the maximum of extensional stresses on the shear rate and stress on the duct wall for narrow-distribution PB and PI. In the figures, the dots indicate the experimental results and the lines, the calculated dependences at $a = 0.5H$. This ratio is determined at some single value of τ_w . One can see that the calculated and experimental data are in satisfactory agreement. Attention is drawn to the linear dependence of $\sigma_{11(\text{max})}$ on $\dot{\gamma}_w$. Moreover, it was found that the dependences $\sigma_{11(\text{max})}(\tau_w)$ are invariant to the molecular mass of the polymers investigated.

Let us further see how the calculated and experimental values of the maxima of extensional stresses agree when we change the reservoir-to-duct width ratio. It should be noted that on changing the duct width the structure of eq. (8) remains intact and only the numerical coefficient of k' is affected.

Figure 11 illustrates the dependence of the value of the maximum of extensional stresses on the shear stresses on the duct wall for a specimen of polymer B for three different values of H_r/H . Here, the dots correspond to the experimental data and the lines, to the calculated ones. The following values of the linear dimension a appearing in eq. (8) were used in the calculation: $a = 0.5H$ for ducts 1 and 2 and $a = 0.1H$ for duct 3. The numerical values of the coefficients k and k' are 1.312 and 1.246, respectively, for duct 1; 1.12 and 1.12 for duct 2; and 1.4 and 1.695 for duct 3.

At low shear stresses one observes a linear relationship between $\sigma_{11(\text{max})}$ and

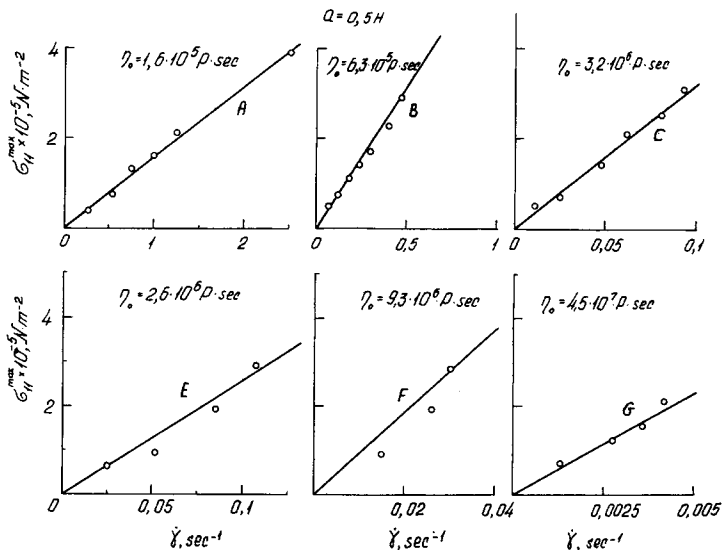


Fig. 9. Dependence of value of maximum of extensional stresses on shear rates on duct wall for samples A, B, C, E, F, and G in duct no. 1: dots, experiment; solid lines, calculation.

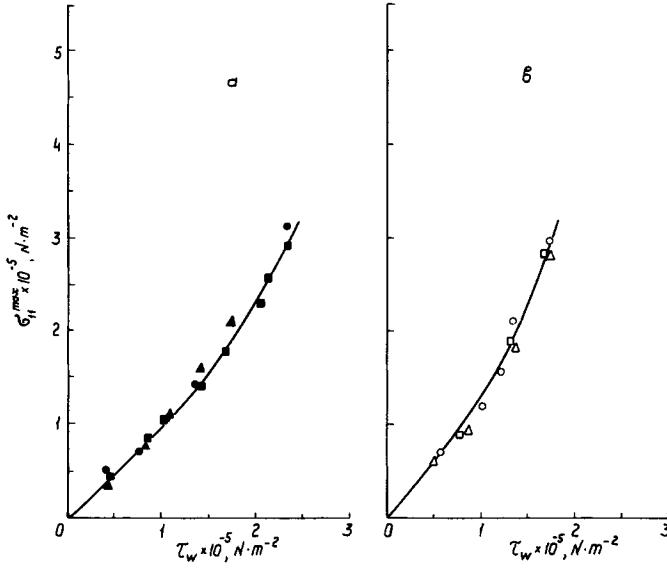


Fig. 10. Dependence of value of maximum of extensional stresses on shear stresses on duct wall for narrow-distribution polybutadienes (a) and polyisoprenes (b): symbols, experiment; lines, calculation. Notation same as in Figure 6.

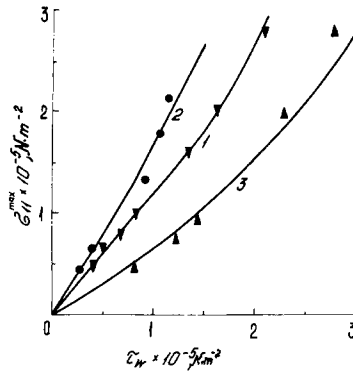


Fig. 11. Dependence of value of maximum of extensional stresses on shear stresses on duct wall for sample B obtained in different ducts: dots, experiment; lines, calculation. Figure correspond to duct numbers in Table II.

τ_w , while at high shear stresses the increase in $\sigma_{11(max)}$ speeds up. This is due to the fact that at high shear stresses a slight deviation from Newtonian behavior is observed, even for narrow-distribution polymers.

It is interesting to estimate the effect of the duct entrance angle α on the change in the distribution pattern of the extensional stresses along the flow axis. Figure 12 presents a comparison of the dependences of $\sigma_{11(max)}$ on Z/H for different angles α during the flow of specimen B. It is seen from these data that the position of a point corresponding to the maximum of extensional stresses is independent of the angle α . At the same time, the distance from the duct edges at which the flow begins to narrow down (and hence the extensional stresses begin to increase) is larger the smaller the angle α . (With a decrease in α the flow narrows down gradually.)

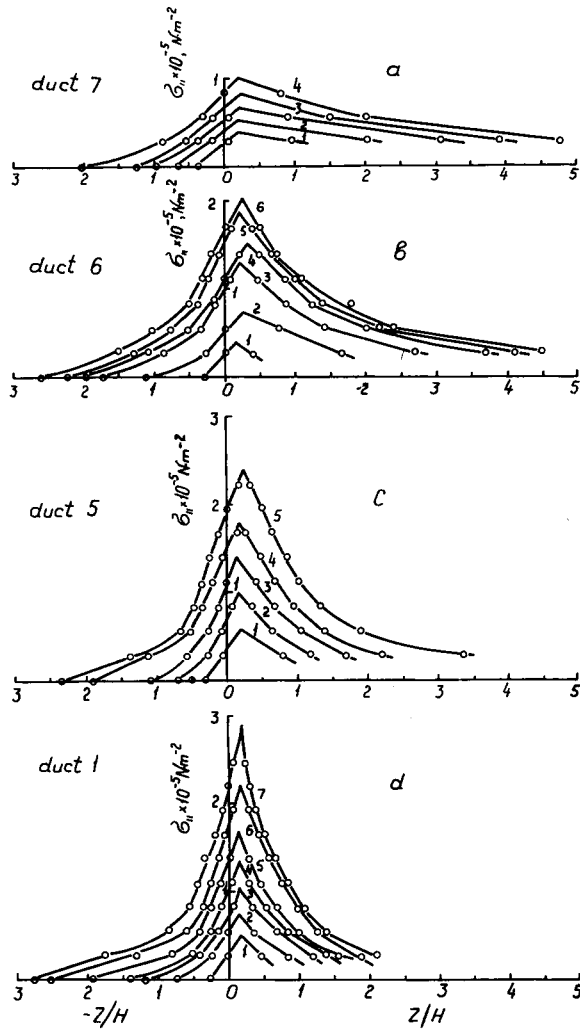


Fig. 12. Curves of distribution of extensional stresses along flow axis in reservoir and inside ducts for sample B. Shear stress on duct wall $\tau_w \times 10^{-5}$, N/m²: (a) (1) 1.51; (2) 11.82; (3) 2.22; (4) 2.40; (b) (1) 0.58; (2) 1.16; (3) 1.70; (4) 1.99; (5) 2.29; (6) 2.4; (c) (1) 0.65; (2) 1.06; (3) 1.41; (4) 1.70; (5) 2.10; (d) (1) 0.43; (2) 0.83; (3) 1.08; (4) 1.33; (5) 1.67; (6) 2.08; (7) 2.22.

Figure 13 shows the dependences of $\sigma_{11(\max)}$ on τ_w for ducts with different shapes of entrance. The solid lines indicate the result of calculation by eq. (8), and the dots, the experimental data. In the upper left-hand corner one can see the relationship between the angle α and the linear dimension a used in the calculations of $\sigma_{11(\max)}$. From the data presented it can be seen that the value of the maximum of extensional stresses can be reduced two- or threefold by changing the duct entrance angle. In addition, it follows that a decrease in entrance angle increases the linear dimension a . This agrees qualitatively with the above-mentioned remark concerning the increase in the length of the region in which the extensional stresses increase with decreasing angle α .

Naturally, a reduction in $\sigma_{11(\max)}$ results in a decrease in the distance Z_0/H over which the extensional stresses relax to zero. Therefore, a decrease in angle α must reduce Z_0/H at the same shear stress. This is illustrated in Figure 14.

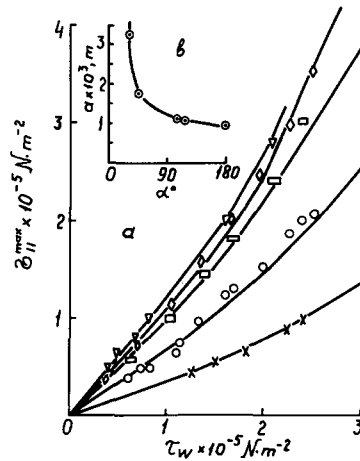


Fig. 13. Dependence of values of maximum of extensional stresses for sample B on shear stress on wall for ducts with different entrance angles (a) and of linear dimension a on entrance angle (b); symbols, experiment; lines, calculation; (∇) 1; (\diamond) 4; (\square) 5; (\circ) 6; (\times) 7. Figures at symbols correspond to duct numbers in Table I.

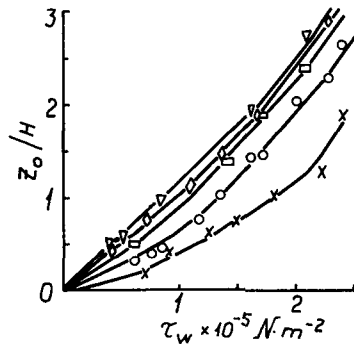


Fig. 14. Dependence of dimensionless distance Z_0/H , corresponding to complete relaxation of extensional stresses, on shear stresses for sample B for ducts with different entrance angles. Notation same as in Figure 13.

In polymer extrusion, the value of the critical shear stress τ_S^1 at which the distortion of the extrudate surface (elastic turbulence) begins to show¹⁷ is of great importance. Figures 15(a) and (b) depict the dependences of the stress τ_S^1 on the duct entrance angle α (a) and on the ratio H_r/H (b). With a decrease in the values of α and H_r/H , τ_S^1 increases.

Hence, it follows that one of the most important causes for flow instability is the high deformation and extensional stress at the duct entrance at which rupture inside the polymer is possible. In the experiments described above, the authors achieved extensional stresses exceeding 10^5 N/m^2 , at which, according to Vinogradov and Rylov,⁹ PB specimens rupture on uniaxial extension. With a decrease in angle α and ratio H_r/H , we have on the one hand a decrease in the maximum of extensional stresses (see Figs. 11 and 13) and, on the other, an increase in shear stresses τ_S^1 at which elastic turbulence sets in (Fig. 15). The increase in τ_S^1 with diminishing α and H_r/H indicates that polymer rupture in the duct entrance may be one of the causes of irregularity in polymer stream.

Thus, the experimental data obtained in the present investigation show that

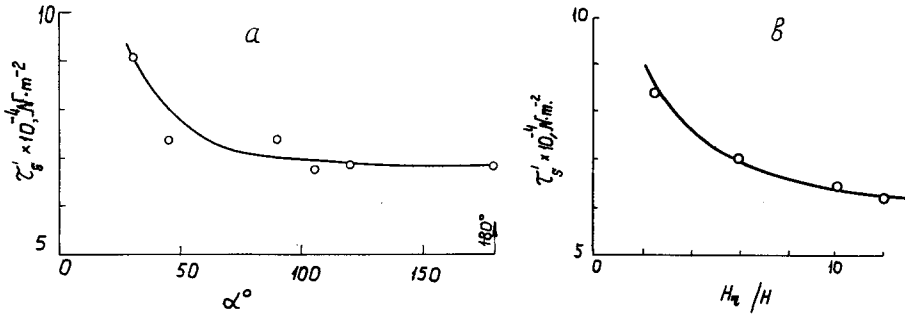


Fig. 15. Dependences for sample B of critical shear stress τ'_s on duct wall on duct entrance angle (a) and on H_e/H ratio (b).

one of the causes for elastic turbulence is the attainment of values of extensional stresses corresponding to the rupture of the material in the preentrance region of the duct. The quantitative polarization-optical description of the processes occurring in the preentrance and entrance regions is in good agreement with the qualitative data known from reference 20.

In the spinning of filaments, the tools are spinnerets, which are capillaries with a small length-to-diameter ratio. Naturally, in the case of polymer flow in a slot with a small L/H , no calculation of stresses and deformation rates is possible; therefore a comparison of the maxima of extensional stresses for different L/H ratios has to be carried out at constant volume flows of the polymer. This enables one to determine, at least qualitatively, how the value of the maximum of extensional stresses depends on the values of L/H .

Figure 16 shows the dependence of the value of the maximum of extensional stresses on L/H for polymer B at different volume outputs. With a decrease in L/H one observes an increase in the value of the maxima of extensional stresses; if $L/H \geq 7$, the indicated value ceases to depend on L/H .

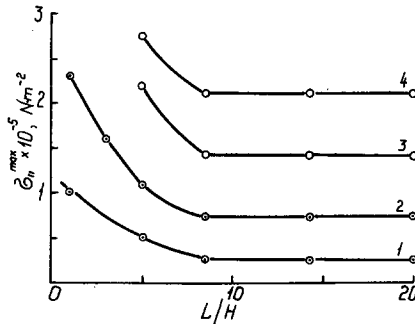


Fig. 16. Dependence of value of maximum of extensional stresses on L/H ($H = 2 \times 10^{-3}$ m) for sample A at $Q \times 10^6 \text{ m}^3/\text{sec}$: (1) 7.8; (2) 17.4; (3) 33.9; (4) 46.5.

References

1. T. R. Fields and D. C. Bogue, *Trans. Soc. Rheol.*, **12**, 39 (1968).
2. C. D. Han and L. H. Drexler, *J. Appl. Polym. Sci.*, **17**, 2329 (1973).
3. F. N. Cogswell, *Rheol. Acta*, **8**, 187 (1968).
4. H. Giesecus, *Rheol. Acta*, **8**, 411 (1969).
5. C. D. Han, R. U. Kim, C. R. Huang, and M. Siscovic, *Polym. Prepr.*, **13**, 986 (1972).
6. F. N. Cogswell, *Trans. Soc. Rheol.*, **16**(3), 383 (1972).

7. F. N. Cogswell, *Polym. Eng. Sci.*, **12**, 64 (1972).
8. G. V. Vinogradov, *Rheol. Acta*, **14**, 942 (1975).
9. G. V. Vinogradov and E. E. Rylov, *Trudy VI Vsesoyuznoy konferentsii po polyarizatsionno-opticheskomu metodu issledovaniya napryazheniy* (Trans. VI (USSR Conf. on Polarization-Optical Method of Stress Research), Leningrad State University Press, 1971, p. 19).
10. V. I. Brizitsky, G. V. Vinogradov, A. I. Isayev, and Y. Y. Podolsky, *J. Appl. Polym. Sci.*, **19**, 25 (1976).
11. M. M. Frocht, *Photoelasticity*, Vol. 1, Wiley, New York, 1941.
12. A. B. Metzner, E. A. Uebler, and C. N. Fong, *A. I. Ch.E.J.*, **15**, 750 (1969).
13. L. H. Drexler and C. D. Han, *J. Appl. Polym. Sci.*, **17**, 2355 (1973).
14. H. Markovitz, in *Rheology, Theory, and Application*, Vol. 4, F. K. Eirich, Ed., Academic Press, New York, 1967, p. 403.
15. A. I. Isayev, *J. Polym. Sci., Phys. Ed.*, **11**, 2123 (1973).
16. P. L. Flory, *Statistical Mechanics of Chain Molecules*, Wiley, New York, 1969.
17. G. V. Vinogradov, A. Y. Malkin, Y. G. Yanovsky, E. K. Borisenkova, B. V. Yarlykov, and G. V. Berezhnaya, *J. Polym. Sci. A2*, **10**, 1061 (1972).
18. G. V. Vinogradov, A. I. Isayev, V. I. Brizitsky, Y. Y. Podolsky, A. Y. Malkin, and M. P. Zabugina, *Mekhanika Polim.*, **6**, 987 (1976).
19. J. M. McKelvey, *Polymer Processing*, Wiley, New York, 1962.
20. P. L. Clegg, in *Rheology of Elastomers*, P. Masons and N. Wookey, Eds., Pergamon Press, New York, 1957, p. 174.

Received March 24, 1977